

# Particle motion and sediment transport over bedforms

R.C. Terwisscha van Scheltinga

*Department of Civil and Environmental Engineering, University of Auckland, Auckland, New Zealand*

G. Coco

*School of Environment, University of Auckland, Auckland, New Zealand*

H. Friedrich

*Department of Civil and Environmental Engineering, University of Auckland, Auckland, New Zealand*

**ABSTRACT:** The processes underlying sediment transport at grain scale are not fully understood. A method to scale down the mechanics from stream reach to bedforms and further to grains and vice versa, remains to be developed. In this study we recorded sediment transport over bedforms and initial sand waves in a laboratory study, in unsteady and non-uniform conditions. High-frequency imaging was used to obtain local measurements of the flux. Importantly, flow patterns and sediment transport were not disturbed during the measurement recordings. Particle velocities were measured using particle image velocimetry (PIV) and the volume of particles in motion is determined from a combination of image processing methods. Transport increases over the bedform. We quantify the variations over different dune shapes and sizes, and perturbations from superposed features. The observed variability in the local sediment fluxes indicate that the transport quickly responds to the unsteady and non-uniform flow over the bed.

## 1 INTRODUCTION

### 1.1 *Sediment transport in non-uniform flow*

At the time-averaged, and reach-averaged scale, sediment transport is determined in bulk fluxes. The depth-slope product predicts the bedload transport, and the commonly used formulas to describe bed load transport in a turbulent flow are a function of the excess shear stress to the power of roughly 1.5 (Kleinhans, 2005; Lajeunesse et al. 2010; Wong & Parker, 2006). The temporal and spatial components of sediment transport by dunes is little understood in relation to average transport (Reesink et al. 2018; Yager et al. 2018). We know more about sediment transport over other roughness elements. Nelson et al. (1995) simultaneously measured sediment transport and streamwise and cross-stream flow in nonuniform and unsteady flow, behind a 0.04 m step. The correlation between streamwise velocity and sediment transport is the strongest, and they measure the strongest correlation (0.5-0.6), with 0.1 s time lag. The correlation with streamwise velocity is stronger than the correlation of sediment transport with (Reynolds) shear stress at 5 mm above the bed. Behind a step, and a distance greater than ~10 steps, bed shear stress becomes nearly constant. For this region, the internal boundary layer, as well as the overlying wake, still develop. The near-bed turbulence structure continues to evolve (Nelson et al. 1995). The frequency and intensity of the near bed turbulence structures are different behind a step. Turbulence structures move a lot of sediment and cause local peaks in bedload transport downstream of a reattachment point.

### 1.2 *Objectives*

Although the measurements described in (Nelson et al. 1995) were performed on fixed steps, they are indicative for how dune crests affect sediment transport. The question arises whether sediment

transport shows similar patterns behind actively migrating 3D bedforms, compared to fixed and simplified dune shapes? New tools and data can help to shed light into the complex processes associated with sediment transport in the presence of migrating 3D bedforms. Through-water photogrammetry using SfM was used to measure detailed 3d-topography in the laboratory and track migrating dunes (Terwisscha van Scheltinga et al. 2020). Whereas high-frequency imaging at close range can be used to measure particle motion at the scale of grains (Drake et al. 1988; Lajeunesse et al. 2010; Radice et al. 2006; Roseberry et al. 2012; Terwisscha van Scheltinga et al. 2019). In this study we describe some observed variations over different dune shapes and sizes.

## 2 METHODOLOGY

### 2.1 *Experimental settings and data acquisition*

Flume experiments took place in a 11.9 m long and 0.44 m wide flume. Different flow conditions were tested. We present results from experiments with mean flow velocity of 0.43 m/s and water depth of 0.18 m. Two cameras were used for data acquisition. One camera recorded overlapping images of the sediment bed, while the flow was paused. The overlapping images were processed into point clouds using photogrammetry (Westaway et al. 2001; Westoby et al. 2012) into a digital elevation models (DEMs). Another camera was used to record the particle motion during the periods of flow over the dunes, and recorded an area of approximately 0.4 by 0.4 m. The camera was moved over the bedforms to record different bed sections.

### 2.2 *Particle velocity and concentration*

Particle concentration was estimated from images of difference, that showed which particles moved position between subsequent images. This method is introduced in Radice et al. (2006) and we developed it further for our experiments. Average particle velocities were calculated from the images of difference using PIV (Terwisscha van Scheltinga et al. 2019) and one velocity vector for every  $0.02 \times 0.02$  m in the image was obtained for every  $1/12$  s during 20 s of data recording for each location. Derivation of particle flux from the measurements of particle velocity and concentration is explained in Figure 1. Particle flux measurements were compared to the dune flux and showed that the particle concentration in our measurements is underestimated. Consistent particle flux underestimation is observed in all recorded images, as not all particles that are moving could be identified. Some particles are too small to measure, and particles that are moving closely together make it more difficult for concentration calculation. We were not able to reliably detect the size of each particle and use the median particle volume for calculation of the particle concentration.

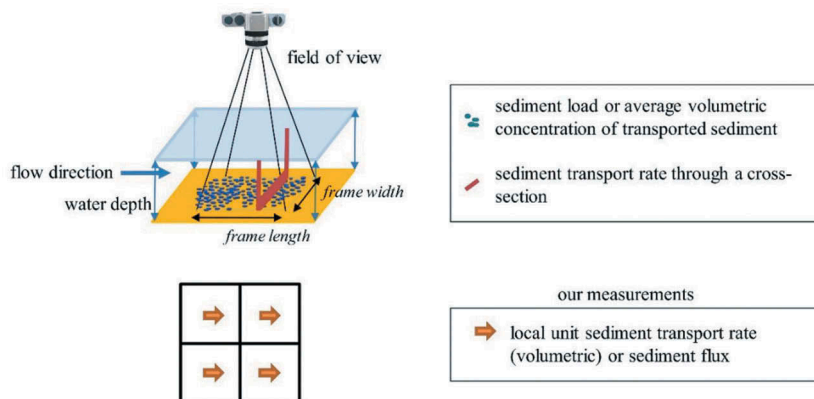


Figure 1. Sketch of measurement of volumetric sediment load by high-frequency image capturing from top-view. Description of derivation of sediment flux ( $q_b$ ) is given.

### 3 RESULTS

Five subsequent measurements were done in time, over a plane bed and with an initial sand wave (small emerging bedform) developing from 0.005 to 0.015 m height. The sand wave grew in several minutes from plane bed, into a lobe crest, and then formed a double crest with a downstream ridge (Figure 2). Particle velocity, particle concentration and particle flux were



Figure 2. Temporal evolution of an emerging bedform from top view. Flow is left to right and mean flow velocity is 0.43 m/s, the water depth is 0.18 m and the bed slope is 0.0010 m.

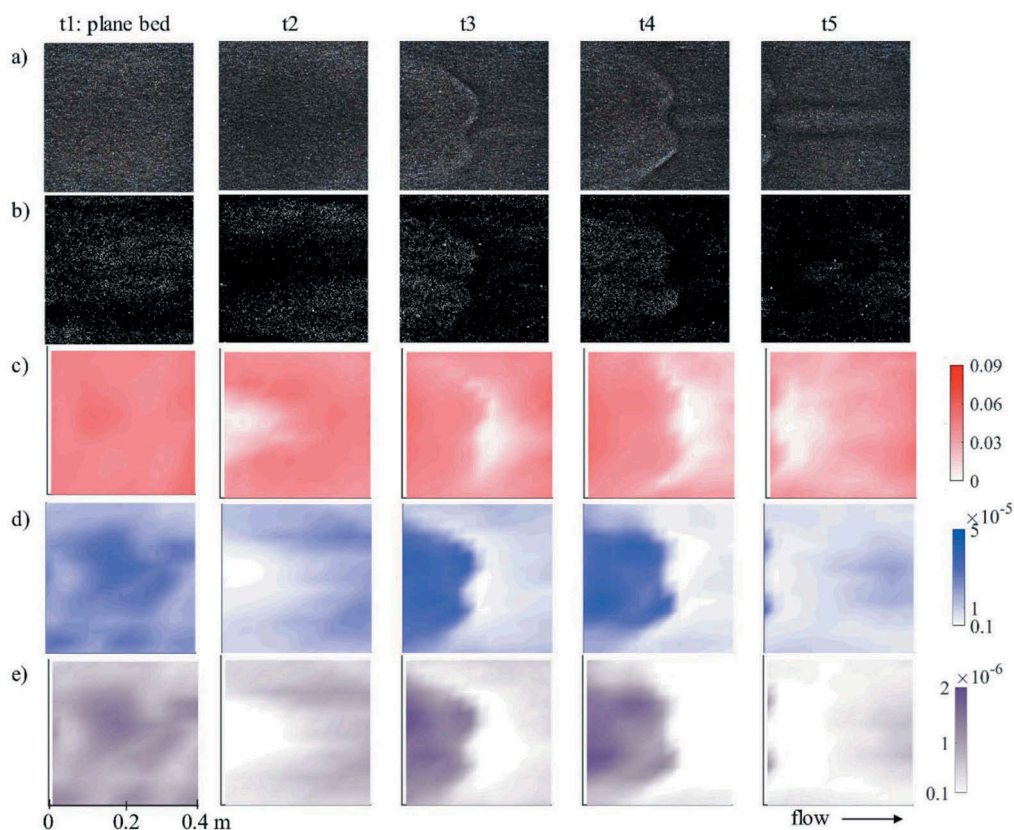


Figure 3. Top view image of the sand bed (a), image of difference with moving particles in white (b) measurements of particle velocity in m/s (c), particle concentration in  $\text{m}^3$  per unit area (d) and particle flux in  $\text{m}^2/\text{s}$  per unit area (e). Measurements are taken over a plane bed (t1) and with an emerging bedforms (t2 – t5). At t1 the sand bed is plane, at t2 there exist a small bedform at the far-left side of the measurements, at t3 and t4 the bedform is visible, and t5 is taken in the lee of the emerging bedform of t4. Mean flow velocity is 0.43 m/s, the water depth is 0.18 m and the bed slope is 0.0010 m.



Figure 4. Reconstructed topographic model of the sand bed with the emerging bedform after  $t_5$ , using through-water SfM. The height of the emerging bedform is 0.015 m. Side walls of the flume are presented for scaling.

measured at five different times, while the sand wave was developing into a bedform. Measurements in Figure 3 show that at plane bed ( $t_1$ ), the mean particle velocity is 0.043 m/s and varies locally between 0.039 m/s (D10) and 0.050 m/s (D90). In the lee of the emerging bedform ( $t_2$ ), only a few particles are moving. At the edges of the bedform, the observed particle velocity is similar to plane bed conditions, whilst particle concentration is a slightly reduced. Over the emerging bedform at  $t_3$  and  $t_4$ , particle velocity is again similar to plane bed conditions, although particle concentration is higher. At  $t_5$ , measurements are taken in the lee of the bedform, after it developed into a double crest and is now higher than at  $t_2$ . The particle velocity and concentration are low, and the affected area is approximately 0.35 m in length for an emerging bedform of 0.015 m (measured using SfM on through-water images, Figure 4). We observe that a small bedform affects the sediment transport considerably, as well as causing an increase in the occurrence of turbulence events, such as sweeps in the lee of the bedform. We counted an increase of turbulence events, from 1 event, to 4, 11, 19 and 28 events during the development from  $t_1$  to  $t_5$ . This shows that turbulence events temporarily increase the particle concentration and particle velocities.

## 4 DISCUSSION

### 4.1 Superposition

Bedforms are important features, and superposed bedforms cause strong local gradients in particle flux. Over a dune slope, the flow is accelerating. It is challenging to compare a particle flux with and without superposed bedforms, in the presence of dune slopes. We use measurements over a plane sediment bed and over an initial sand wave developing into a bedform, which help to explore the effect of superposed features with a height of 0.01-0.02 m. We measured higher particle concentration over the emerging bedform, as compared to a plane bed. Particle velocities are more similar. In the lee of the bedform, particle velocity and concentration increase gradually from zero, and accelerate over a distance of 0.35 m for the tested flow condition.

### 4.2 Turbulence events

In the lee of the superposed form, transport is low and affected by turbulence events that become more frequent while the bedform grows. These events are associated with the separation and reattachment process (Nelson et al. 1995). For the sequence we measured, the turbulent events were negligible in terms of sediment flux for  $t_1$  and  $t_2$ , but not for  $t_3$  to  $t_5$ .

According to our observations, the turbulence events occurred mostly over the ridge in t5 and are likely enhanced by the shape of the upstream bedform. They were very frequent for a double crest. This suggests that the shape of a superposed bedform is important, not only for turbulence generation, but also for quantifying sediment transport dynamics.

#### 4.3 *Sediment transport behind a step*

Previous measurements of the flow behind a fixed step of 0.04 m and water depth of 0.2 m showed that the mean flow had recovered at a distance of 20-25 times the step height (Nelson et al. 1995). We can deduce from the transport flux in Figure 3 (t5) that the flux is similar to that one of plane bed conditions after a distance of approximately 0.35 m (ignoring the measurements near the side wall). The distance is at  $0.35/0.015 = 23$  times the step height. Observing this similarity needs further assessment, with the bedform generated in our experiments being smaller and migrating, as compared to the processes observed for fixed steps previously.

#### 4.4 *Bedform growth*

We observe that the emerging bedform increased the transport capacity, as compared to plane bed conditions. In terms of local sediment transport gradients, a positive gradient contributes to the erosion of the bed over the stoss slope for an emerging bedform. Most of the sediment is deposited, as it reaches the lee slope. Downstream of the lee face, transport is close to zero and increases gradually. This gradient also causes local bed erosion. The transport gradients measured over the emerging bedform translate into a growing bedform, and the sediment transport downstream of the bedform is affected over a distance of at least 20 step heights. Our measurements over an emerging bedform indicate that superposed features on the sand bed, even though they are small, affect sediment transport dynamics locally and temporally.

### 5 CONCLUSIONS

Images were used to measure the particle motion and the 3D morphology of an emerging bedform (initial sand wave). The sediment transport measurements over the small emerging bedform showed an increase in particle concentration as compared to plane bed conditions, with particle velocities being more similar. The local gradients were strong and the transport gradually increases over the emerging bedform. The observed flux is similar to plane bed conditions after approximately 23 step heights, which is comparable to observations behind a larger fixed step. The emerging bedform compared in size to superposed features, as observed on dune slopes. The shape and size of the superposed bedforms are affecting the frequency of turbulence events.

### REFERENCES

- Drake, T. G., Shreve, R. L., Dietrich, W. E., Whiting, P. J. & Leopold, L. B. 1988. Bedload transport of fine gravel observed by motion-picture photography. *Journal of Fluid Mechanics*, 192, 193–217.
- Kleinhans, M. G. 2005. Flow discharge and sediment transport models for estimating a minimum time-scale of hydrological activity and channel and delta formation on Mars. *Journal of Geophysical Research: Planets*, 110 (E12), n/a-n/a.
- Lajeunesse, E., Malverti, L. & Charru, F. 2010. Bed load transport in turbulent flow at the grain scale: Experiments and modeling. *Journal of Geophysical Research: Earth Surface*, 115(4).
- Nelson, J. M., Shreve, R. L., McLean, S. R. & Drake, T. G. 1995. Role of Near-Bed Turbulence Structure in Bed Load Transport and Bed Form Mechanics. *Water Resources Research*, 31(8), 2071–2086.
- Radice, A., Malavasi, S. & Ballio, F. 2006. Solid transport measurements through image processing. *Experiments in Fluids*, 41(5), 721–734.
- Reesink, A. J. H., Parsons, D. R., Ashworth, P. J., Best, J. L., Hardy, R. J., Murphy, B. J., McLelland, S. J. & Unsworth, C. 2018. The adaptation of dunes to changes in river flow. *Earth-Science Reviews*, 185, 1065–1087.

- Roseberry, J. C., Schmeeckle, M. W. & Furbish, D. J. 2012. A probabilistic description of the bed load sediment flux: 2. Particle activity and motions. *Journal of Geophysical Research: Earth Surface*, 117(3).
- Terwisscha van Scheltinga, R. C., Coco, G., Kleinhans, M. G. & Friedrich, H. 2020. Observations of dune interactions from DEMs using through-water Structure from Motion. *Geomorphology*.
- Terwisscha van Scheltinga, R. C., Friedrich, H. & Coco, G. 2019. Sand particle velocities over a subaqueous dune slope using high-frequency image capturing. *Earth Surface Processes and Landforms*.
- Westaway, R. M., Lane, S. N. & Hicks, D. M. 2001. Remote sensing of clear-water, shallow, gravel-bed rivers using digital photogrammetry. *Photogrammetric Engineering and Remote Sensing*, 67(11), 1271–1281.
- Westoby, M. J., Brasington, J., Glasser, N. F., Hambrey, M. J. & Reynolds, J. M. 2012. ‘Structure-from-Motion’ photogrammetry: A low-cost, effective tool for geoscience applications. *Geomorphology*, 179, 300–314.
- Wong, M. & Parker, G. 2006. Reanalysis and correction of bed-load relation of Meyer-Peter and Müller using their own database. *Journal of Hydraulic Engineering*, 132(11), 1159–1168.
- Yager, E. M., Venditti, J. G., Smith, H. J. & Schmeeckle, M. W. 2018. The trouble with shear stress. *Geomorphology*, 323, 41–50.